Vibrational Spectra of Liquid Interfaces with A 100 kHz Sub-1 cm^{-1} High Resolution Broadband Sum Frequency Generation Vibrational Spectrometer (HR-BB-SFG-VS)

Jing-Ming Cao, [†, ‡] An-An Liu, [‡] Shu-Yi Yang, [†, ‡] Xing-Xing Peng, [‡, ¶] and Hong-Fei Wang*[, ‡, ¶]

[†] Department of Chemistry, Zhejiang University, Hangzhou, 310027, Zhejiang Province, China

[‡]Department of Chemistry, School of Science, Westlake University, Hangzhou, 310030, Zhejiang Province, China

[¶] Institute of Natural Sciences, Westlake Institute for Advanced Study, Hangzhou, 310030, Zhejiang Province, China

Corresponding Author

*(H.-F. Wang) E-mail: wanghongfei@westlake.edu.cn

ORCID

Jing-Ming Cao: 0009-0007-6395-5516

An-An Liu: 0009-0001-8191-6111

Shu-Yi Yang: 0009-0000-9138-4609

Xing-Xing Peng: 0000-0003-1468-2770

Hong-Fei Wang: 0000-0001-8238-1641

ABSTRACT

Sub-1 cm^{-1} high-resolution broadband sum-frequency generation vibrational spectrometer (HR-BB-SFG-VS) using synchronized picosecond and femtosecond lasers at 1 kHz was first reported over a decade ago, and many advantages of the HR-BB-SFG-VS over the conventional BB-SFG-VS have been well-documented. A high-efficient and low-cost version of the HR-BB-SFG-VS is needed for broader adoption of this powerful interface specific spectroscopic technique. Here, we report the realization of such a sub-1 cm^{-1} HR-BB-SFG-VS with a tunable repetition rate around 100 kHz. Instead of synchronization of an additional expensive 90 picosecond laser for enough power to achieve high spectral resolution SFG measurement, a chirped volume Bragg grating (CVBG) is implemented with the second harmonic band compression (SHBC) unit to generate an intense 90 picosecond laser pulse at 517 nm with a bandwidth of about 0.16 cm^{-1} from a 150-fs laser pulse at ~1034 nm, with an efficiency of ~26%. The effectiveness of this new SFG system is demonstrated through the SFG spectra obtained with a spectral resolution of 0.6 cm^{-1} and excellent lineshape from the air/DMSO aqueous solutions interfaces, and the air/water interface, without apparent surface heating effect. This development provides a low-cost and easy-to-implement powerful HR-BB-SFG-VS instrumentation for broad applications in structure and dynamics studies on the illusive molecular surfaces and interfaces.

TABLE OF CONTENTS (TOC) GRAPHICS

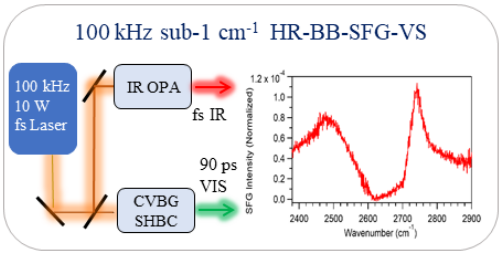

1. Introduction

Sum-frequency generation vibrational spectroscopy (SFG-VS) have been proven the powerful spectroscopic technique to interrogate the spectroscopy, structure, and dynamic interactions on the molecular surfaces and interfaces, particularly liquid interfaces, in the past three dozen years.[1-4] Quantitative information of molecular interfaces can be analyzed in details with the ability to obtain higher quality SFG-VS spectra with spectral, polarization, incident angle and phase resolutions. [4-9]

Sub-1 cm^{-1} high-resolution broadband sum frequency vibrational spectroscopy (sub-1 cm^{-1} HR-BB-SFG-VS) with a spectral resolution of 0.6 cm^{-1}, the highest spectral resolution so far, was achieved in 2011 by synchronizing a ~90 picosecond (ps) laser and a ~35 femtosecond (fs) laser at the repetition rate of 1 kHz.[10] In this apparatus, the ~90 ps 800 nm laser pulse with pulse energy up to 3.5 mJ has a less than 0.2 cm^{-1} bandwidth, and the ~35 fs 800 nm laser pulse up to 7 mJ was used to generate broadband middle IR pulses with more than 260 cm^{-1} FWHM (full width at half-maximum) bandwidth.[10] Taking the advantages of the multiplexing measurement in the conventional BB-SFG-VS and sub-1 cm^{-1} spectral resolution, the sub-1 cm^{-1} HR-BB-SFG-VS provides accurate and nearly intrinsic SFG spectral lineshape with much better signal-to-noise ratio (SNR), and without spectral distortion as in the conventional BB-SFG-VS.[10-11]

The advantages of the sub-1 cm^{-1} HR-BB-SFG-VS over the conventional BB-SFG-VS, typically with ~10 cm^{-1} or more spectral resolution, has been well demonstrated and understood.[7, 12-18] In conventional BB-SFG-VS, the visible pulse usually has a pulse width of 1-2 ps and therefore a spectral resolution of ~10 cm^{-1} or more. Such visible pulses of a few picoseconds cannot effectively cover the coherence time of the molecular vibrational motions typically last for many picoseconds. This leads to the truncation of the up-converted SFG field in the time domain, and unavoidably translates into lineshape distortion and spectral broadening in conventional BB-SFG-VS.[19] Not only does such visible pulse lead to significant spectral broadening and distortion of the SFG spectra, but also the uncontrolled chirping in such visible pulse can lead to additional spectral peak shifts and

distortion, further complicating the analysis of the SFG spectra.[4, 18] Supposedly, with these advantages, sub-1 cm^{-1} HR-BB-SFG-VS should have replaced the conventional BB-SFG-VS in practice. Despite, the requirement of the sub-1 cm^{-1} HR-BB-SFG-VS to synchronize an additional long picosecond laser to the sub 100 fs laser makes the sub-1 cm^{-1} HR-BB-SFG-VS system not only much more costly (usually close to 1M US$), but also requires much more laboratory space, i.e. the optical table needs to be more than twice as big as that for the conventional BB-SFG-VS. These factors made the sub-1 cm^{-1} HR-BB-SFG-VS hard to be adopted in most laboratories. So-far, there are only two known sub-1 cm^{-1} HR-BB-SFG-VS systems using the synchronization approach as reported.[10, 20] In comparison, the SFG-VS field is still dominated with the conventional BB-SFG-VS, and with a few systems with somewhat improved spectral resolution closer to 1 cm^{-1}, despite its lower resolution and less desirable spectral lineshape broadening and distortion due to the lower spectral resolution of the conventional BB-SFG-VS, since it was first introduced in 1998.[15]

Up to now, most conventional BB-SFG-VS employed laser systems with repetition rate of 1 kHz.[21-24] BB-SFG-VS with 5 kHz with about 1.4 cm^{-1} resolution, and 10 kHz with about 5 cm^{-1} resolution was also reported.[25-26] There were also a few reports of BB-SFG-VS spectrometers operating at a repetition rate around 100 kHz on air/solid interface, with spectral resolution around 3 cm^{-1}.[27-28] Most recently, EKSPLA reported a ready-to-announce commercial fiber laser and dual-amplifier based high-resolution BB-SFG-VS with a ~3 cm^{-1} spectral resolution running at 10 kHz with a dual amplifier.[29] Modelling of laser heating effects on liquid surface showed that when the repetition rate is above 1 kHz, the heating effects essentially resembles the case of the CW laser with the same power.[30] Heating up the liquid interface has always been a practical issue in SFG-VS experiment.[31] As far as we have known, there has been no 100 kHz SFG-VS measurement reported for measurement on liquid interface,[32] except for the phase-resolved heterodyne measurement on the charged silica/water interface with a spectral resolution about 25 cm^{-1}.[33] It is possibly due to the fact that heating effects need additional attention and harder to control in the experiments with higher IR laser powers, as the average IR laser power for a 100 kHz system is usually 100 or 10 times higher than

that of the 1 kHz system with similar or one order higher energy per pulse, respectively.

The principles and advantages for sub-1 cm^{-1} HR-BB-SFG-VS has been fairly well understood and firmly established.[4, 7, 34] An effective sub-1 cm^{-1} HR-BB-SFG-VS system needs a sub-1 cm^{-1} visible laser pulse for the spectral resolution and a broad enough infrared (IR) laser pulse for spectral coverage.[10, 15, 19] The key for the success is to generate sub-1 cm^{-1} visible (or near-infrared) laser pulse with strong enough pulse energy to generate detectable SFG signal. If the visible and IR pulses are generated from the same laser source, they can be directed to the surface simultaneously to generate the SFG signal. This is the case in the conventional BB-SFG-VS, and the scanning SFG-VS. However, to generate a sub-1 cm^{-1} visible laser pulse, which is with a time width of ~15 ps for a transform-limited Gaussian pulse, or much longer than 15 ps if not transform-limited,[34] from a broad sub 100 fs laser pulse (usually more than 150 cm^{-1} broad), is very inefficient energy-wise. Typically, with the 4f pulse-shaping scheme as used in many conventional BB-SFG-VS, only about 1/150 of the total energy can be used to take a less than 1 cm^{-1} band from the broadband of 150 cm^{-1} of the stretched 100 fs visible pulse, not enough to generate SFG signal for effective detection in most cases. This is why the spectral resolution in the conventional BB-SFG-VS is typically 10 cm^{-1} or more.[11] There are a few SFG-VS works using second-harmonic band compression (SHBC) to generate narrow band visible light from the 100 fs broadband pulse with an efficiency as high as 25%.[26, 32] Typically, in the SHBC approach, a short femtosecond visible pulse is splitted into two beams, both stretched into multiple picoseconds, and the group velocity dispersions (GVD or chirping) of the two pulses are fine-tuned in opposite directions with a pair of grating-based dispersive units (GBDU), respectively, before being sent into a doubling crystal to generate picosecond pulses in the second harmonic wavelength with significantly compressed bandwidth.[32] In principle, if the two pulse are stretched long enough and their chirps are controlled ideally, it would have been possible to generate SHBC pulses with sub-1 cm^{-1} band width. Therefore, the SHBC approach seems to be much more promising in achieving better spectral resolution, possibly with sub-1 cm^{-1} spectral resolution, and with enough pulse energy for SFG-VS measurement. However, using GBDU to accurately control the stretches

and the chirps of the two pulses for generating the sub-1 cm^{-1} narrow bandwidth in SHBC may take tremendous efforts. The resolution reported so far for SHBC in SFG-VS is no better than 3 cm^{-1}.[28, 32, 35] Until now, synchronization of a picosecond and a femtosecond lasers systems at 1 kHz remains the only successful approach for sub-1 cm^{-1} HR-BB-SFG-VS.[4, 7, 10-11, 19, 34, 36-39]

Recently, it has been demonstrated that well-designed chirped volume Bragg gratings (CVBG), a small piece of precision optical device consists of multiple photorefractive glass plates, can be used to stretch femtosecond pulses into ~100 ps pulses with well-tuned large positive and negative group velocity dispersions (GVD). A pair of such pulses with opposite GVDs (chirps) can be used to generate second harmonic pulses with bandwidth well below sub-1 cm^{-1} through the SHBC processes.[40-42]

In this work, we report a 100 kHz sub-1 cm^{-1} HR-BB-SFG-VS with SHBC using the CVBG technology. With CVBG and SHBC, intense ~100 picosecond laser pulses at 517 nm (with a bandwidth of about 0.16 cm^{-1}) was successfully generated from 150 fs laser pulses at 1030 nm, with an efficiency of ~ 26% out of the total input energy, ensuring narrow enough bandwidth and strong enough energy for sub-1 cm^{-1} HR-BB-SFG-VS measurement. With this sub-1 cm^{-1} HR-BB-SFG-VS system, we successfully measured the sub-1 cm^{-1} resolution SFG spectra of the air/DMSO aqueous solutions interfaces, and the air/D_2O interface with a resolution of ~0.6 cm^{-1}. The power densities of the visible and IR pulses were carefully controlled to achieve about 3 times of the signal of that of the HR-BB-SFG-VS system with synchronized ps and fs lasers. Furthermore, no apparent surface heating effect was observed even for the air/D_2O interface which has a three orders smaller signal than the air/DMSO interface, making this 100 kHz SFG system sensitive and reliable enough to be applied to other liquid interfaces. This sub-1 cm^{-1} HR-BB-SFG-VS system is cost-effective, highly-efficient, less space-demanding, and the spectra obtained are with high SNR, making it highly adoptable in laboratories for surface and interface spectroscopy structure and dynamics studies. The same CVBG technology can also be readily extended to other multiplex nonlinear optical spectroscopies into the sub-1 cm^{-1} resolution regime, such as the femtosecond stimulated Raman

spectroscopy (FSRS) and the coherent anti-Stokes Raman spectroscopy (CARS), etc.

2. Experiments

Experimental setup. The 100 kHz sub-1 cm^{-1} HR-BB-SFG-VS is based on a 10 Watts, 150 fs and 1030 (± 10) nm femtosecond Yb:KGW tunable repetition-rate laser system (Pharos, Light Conversion, Ltd., Lithuania). It can also be constructed using other similar laser systems with much less cost, such as femtosecond fiber lasers with slightly different parameters, or with higher pulse energy for pump-probe SFG-VS experiment. Such effort is underway in our laboratory. Figure 1 is the schematic drawing of the system including the laser system, the second harmonic band compression (SHBC) unit for sub-1 cm^{-1} picosecond pulse generation, the optical parametric amplifier (OPA) unit for broadband IR generation, and the HR-BB-SFG-VS unit for SFG-VS experiment. The 10 Watts 1030 nm 150 fs laser beam out of the Yb:KGW laser system is polarized vertically (*p*-polarized), and is rotated into 45° polarization using a half-wave plate (HWP1). Then, a thin film polarizer (TFP) splits the power of this laser beam equally to pump the SHBC unit and the OPA unit, respectively. The whole experimental setup can be easily accommodated on a 3*1.5 m optical table, available in most laser laboratories.

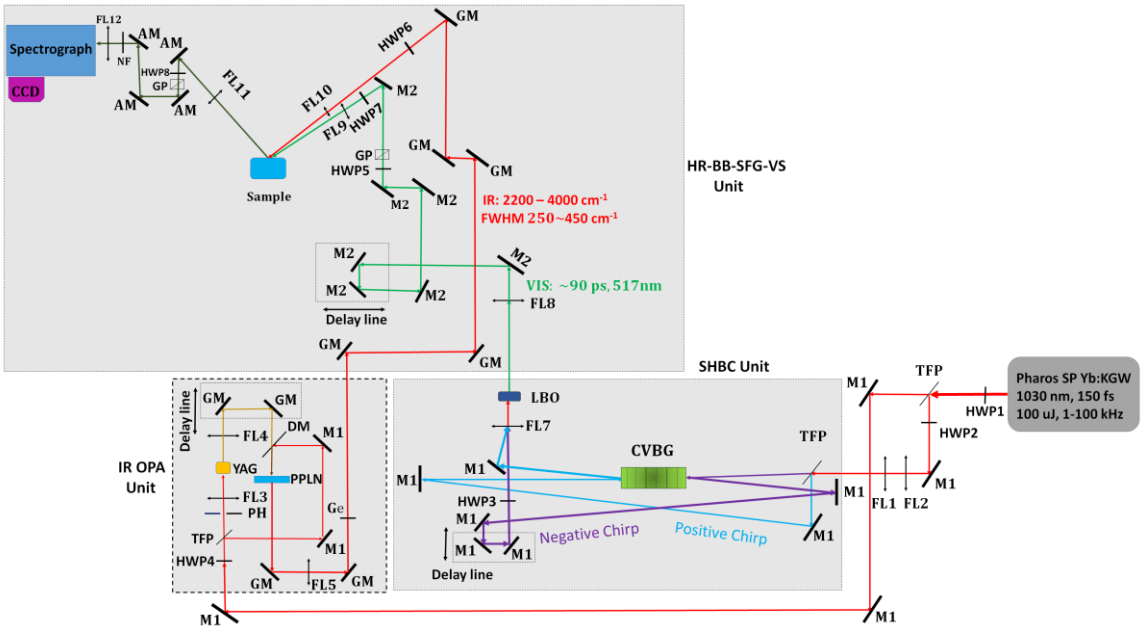

Figure 1. Experimental setup of the 100 kHz sub-1 cm^{-1} HR-BB-SFG-VS. Half of the energy of the 10 Watts 1030 nm Yb:KGW laser is used to generate the ultra-narrowband visible pulse from the SHBC unit using a chirped volume Bragg grating (CVBG), and another half is used to pump an IR optical parametric amplifier (OPA) unit to generate broadband

IR pulses in the range of 2200-4000 cm^{-1}. The visible pulse and the broadband IR pulse are sent to the HR-BB-SFG-VS unit for SFG measurement. M1: dielectric high reflection mirror for 1030 nm; M2: dielectric high reflection mirror for 517 nm; GM: parabolic gold mirror for broadband IR; AM: Aluminum mirror used for SFG signal; DM: dichroic mirror, highly reflective (HR) at 1.03 μm/2.6–3.6 μm, and highly transmitting (HT) at 1.4–1.7 μm; TFP: thin film polarizer, HWP (1-8): half-waveplate, respectively; FL (1-12): focusing lens; PH: pin hole; Ge: Germanium Long pass filter; GP: Glan prism; CVBG: chirped volume Bragg Grating; LBO: crystal for second harmonic generation; YAG: crystal for white light generation; PPLN: periodically poled lithium niobate (PPLN) crystal. All the optics are with the diameter of 25.4 mm from the Union Optics, Inc. China, except those specified.

SHBC Unit using CVBG. The *s* polarized (horizontally polarized) light reflected from the first TFP is rotated into 45º polarization. Then, the beam diameter is reduced with a ratio of 2:1, before being sent into a second TFP for beam splitting into equal power. The beam diameter needs to be reduced because the chirped volume Bragg grating (CVBG, CBG-1035-9, 14*5*5 mm, from the OptiGrate Corp., U.S.A.) only have an aperture of 5 mm. The ~2.5 Watts reflected *s*-polarized beam is guided into the back of the CVBG with an angle smaller than 5º from the long axis [41] with two reflecting mirrors (M1) for 1030 nm to generate a beam with positively chirp. The angle itself is not crucial, but it has to be small enough to enter and exit from the 5*5 mm aperture of the CVBG crystal. The ~2.5 Watts transmitted laser beam with *p*-polarization is directly sent into the CVBG with the same angle from the long axis, and the reflected beam is with negative chirp. This negatively chirped pulse is properly delayed and rotated into s-polarization with a half-wave plate (HWP3) before being combined with the positively chirped beam. Both beams are focused (with focusing lens FL7, FL=250 mm) and are spatially and temporally overlapped on an LBO crystal for second harmonic generation (SHG). The stretching factor of this CVBG (CBG-1035-9) is 9 ps/nm and the maximum stretching time is ~115 ps. Thus, the 150-fs pulse with a bandwidth about 10nm is stretched into a 90 ps pulse with a nearly linear chirp. The laser beam entering the opposite direction of the CVBG is chirped in opposite sign. Thus, with the positively and negatively chirped pulses, the SHG pulse generated from the LBO crystal (Type I, 90°/13.8°, AR coated for 1030 ± 15 nm and 515 ± 15 nm on both sides, size 5*5*5 mm, Fujian Crystoke Photoelectric Technology Co., Ltd, China) has a 90 ps full width at half maximum (FWHM) and is nearly transform-limited. Measurement results in Figure 2 show that the center wavelength of the SHG is 19329.2 ± 0.1 cm^{-1} (517.35 ± 0.01 nm), and the bandwidth measured with a 750 mm focal length spectrograph (Shamrock 750, 1800 l/mm, 500 nm blaze, Andor Co. Ltd.,

UK) is 0.65 ± 0.01 cm^{-1}. The maximum power of the 517 nm light is 1.3 Watts, a 26% conversion efficiency out of the 5 Watts total input power. This provides strong enough power and narrow enough bandwidth for sub-1 cm^{-1} HR-BB-SFG-VS measurement. 0.60 cm^{-1} is about the limit of spectral resolution for our 750 mm spectrograph. The actual line width of the 90 ps pulse can be much narrower than the 0.65 cm^{-1} FWHM shown in Figure 2 if measured with spectrometer with higher spectral resolution. A transform-limited 90 ps pulse has a linewidth of about 0.16 cm^{-1}. In order to be able to measure SFG-VS signal with such linewidth, spectrograph with better resolution is required , and will be implemented in the future.

This approach of using CVBG to generate positive -negative chirped pulse pair is simple and straight forward.[41-42] The time span of the linearly chirped pulse pair is determined by the band width of the input beam times the stretching factor which is specially designed for each CVBG crystal for specific optical wavelength, which is 9 ps/nm for 1030 nm in this work. The FWHM bandwidth of the 150 fs pulse is about 10 nm, resulting a stretched pulse of ~90 ps. Using a 300 fs pulse at 1030 nm may result in a ~45 ps stretched pulse, with a transform-limited band width of ~0.33 cm^{-1}. Therefore, there is a broad room for the CVBG technology be broadly applicable in nonlinear spectroscopy with pulse of mixed time width and band width. As far as we have known, the work reported here is the first time using CVBG technology for nonlinear spectroscopy studies.

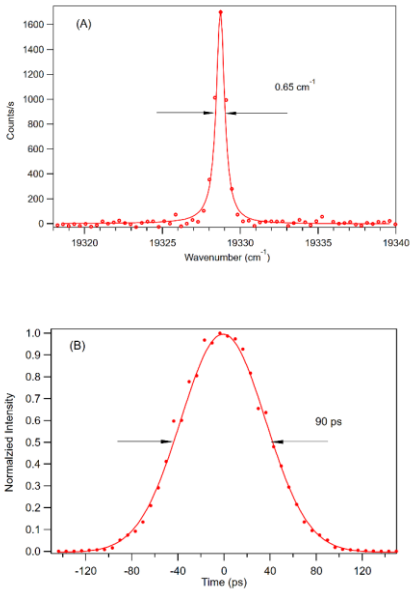

Figure 2. Spectrum (A) and pulse width of the laser pulse generated from the SHBC unit. **Panel A**. The FWHM of visible pulse at 19329.2 ± 0.1 cm^{-1} is 0.65 ±0.01 cm^{-1} fitted with a Gaussian function. **Panel B.** The time profile of the 517.35 ± 0.01 nm pulse measured with SFG cross-correlation measurements with a 150 fs IR pulses. The FWHM is 90.5 ± 0.1 ps fitted with a Gaussian function.

OPA Unit. The OPA unit uses the configuration with one stage optical parametric amplification with a periodically poled lithium niobate (PPLN) crystal, coving ~2200-4000 cm^{-1} (~4550-2500 nm) in the IR range.[27, 32] Similar configuration using a $LiGaS_2$ crystal can extend IR range to ~900-3200 cm^{-1} (~11000-3100 nm).[43] The 5 Watts *p*-polarized beam is used to pump the OPA unit. The *p*-polarized (vertically polarized) light is rotated into polarization angle of 71.6º, making the *s*-to-*p* beam powers with a 90%:10% ratio, and separated the *s* and *p* beams with a TFP. The transmitted *p* polarized light with about 10% power (~50 μJ per pulse) is loosely focused (FL3, 75 mm focal length) on an c-cut YAG plate (5*5*5 mm, CASTECH Inc.) to generate broad supercontinuum light. The supercontinuum light beam is collected with a focal lens (FL4, FL = 500 mm), and guided with two gold mirrors (GM) into the PPLN crystal (AR-coated, 5% MgO-doped fan-out type II, 10*3*3 mm size, HC Photonics Corp., Taiwan, China) for IR frequency generation through the optical parametric amplification (OPA) process in the PPLN crystal, pumped with the *s*-polarized 1030 nm beam with the 90% of the total power. The beam diameter of the supercontinuum beam entering the PPLN crystal is about 125 μm. The supercontinuum beam and the 1030 nm pump beam are combined collinearly using a dichroic mirror (DM, 90% reflection at 1030 nm, and 90% transmission (HT) in the range of 1.2 μm-1.7 μm). By horizontally moving the PPLN crystal and by adjusting the delay time through moving the two GM mirrors, the idler beam with broad IR spectral bands covering the range of ~ 2200-4000 cm^{-1} with bandwidth (FWHM) in the range of 250 to 450 cm^{-1}, respectively, can be generated. This idler beam is guided with a pair of gold mirrors (GM) and collimated with an IR transmitting CaF_2 focal lens (FL4, 200 mm focal length). The idler beam passes through the Ge filter (25.4 mm diameter, 1.5 mm thickness, Edmund, Inc., U.S.A.). Then, it is delivered to the SFG-VS unit using a couple of gold mirrors (GM). Typically, the output power of the OPA unit measured, at the sample without purging of H_2O and CO_2 in the air, is ~200 mW at 100kHz, i.e. 2 μJ per pulse, at

~ 3.3 μm; about 80 mW around 2.5 μm (4000 cm^{-1}); and 40 mW around 4.5 μm (2200 cm^{-1}). The typical IR power and the band profiles are showing in Figure 3. The average power, band position and the FWHM of each band is listed in Table I.

Table I. Broadband IR band energy and profile parameters in Figure 3.

Power (mW)	Position (cm^{-1})	FWHM (cm^{-1})
70	3684	265
130	3539	450
150	3340	285
160	3235	255
185	3141	250
190	3026	250
160	2902	365
150	2750	240
145	2665	240
130	2563	235
120	2495	200
110	2396	93
45	2283	95

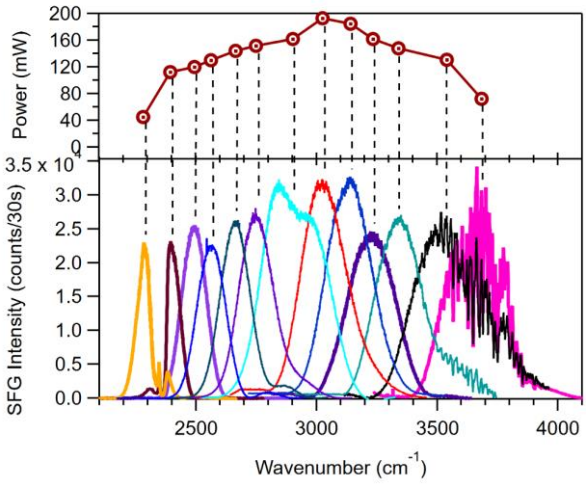

Figure 3. (Upper Panel): Average power of the IR bands from the OPA unit at the sample. (**Lower Panel**): represents the non- IR bands from the OPA unit measured with the non-resonant SFG from z-cut α-quartz reference crystal surface. Purging in the IR beam path is required to remove the absorption of the water and the CO_2 vapors for the IR bands in the 3500-4000 cm^{-1} region and the 2200-2300 cm^{-1} for better SFG measurement.

HR-BB-SFG-VS Unit. The setup of the HR-BB-SFG-VS unit (Figure 1) is similar to typical BB-SFG-VS reported previously.[10] Both the visible and the IR beams are polarization controlled and simultaneously focused on the surface of the sample. The incident angles from the surface normal are 65° for the visible beam and 50° for the IR beam, respectively. To achieve sub-1 cm^{-1} spectral resolution, the SFG signal is collected and delivered into a 750 mm spectrograph (Shamrock 750,

1800 lines/mm 500 blaze grating, Andor Co. Ltd., UK) and recorded with a thermoelectrically cooled (−80℃) Electron-Multiplied CCD (EM-CCD) camera (Newton 971P, back-illuminated, 1600 × 400 pixels, 16 μm^2 pixel size, Andor Co. Ltd., UK). Background signal with a 1 ns delay of the visible pulse against the IR pulse is subtracted from the measured SFG signal. Then, it is normalized to the SFG signal from a thick z-cut quartz (10*10*10 mm, Simona Synthetic Crystals, Co. Ltd., China) reference, oriented in its *x* direction.[10, 44] All data were taken with an entrance slit width of 50 μm of the Shamrock spectrograph. Further reduction of this slit width resulted decrease of the signal level without increasing the spectral resolution.

Typically, a 2-minutes exposure of the CCD camera was used for collecting data for the air/DMSO (Dimethyl Sulfoxide, > 99.7%, No. 472301 from Sigma-Aldrich) and air/ DMSO aqueous solution interfaces, and 10 minutes exposure for the air/D_2O (Deuterium Oxide, > 99%, No. 435767 from Sigma-Aldrich) interface. Distilled water after the treatment of a Millipore purifier (Milli-Q, IQ 7000, Millipore-Sigma) is used for preparing DMSO aqueous solutions.

All measurements are conducted under ambient conditions in a controlled clean room, with the room temperature at 21.0° ± 0.1° and the humidity at < 40%.

3. Results and Discussions

With this new sub-1 cm-1 HR-BB-SFG-VS instrumentation, spectra of the air/DMSO aqueous solution interface and air/D2O interface were successfully obtained. The signal levels of these liquid interfaces differ by three orders of magnitude, and their spectra are with excellent signal-to-noise ratio (SNR) and are without observable heat effect. In addition, with the sub-1 cm^{-1} spectral resolution, novel phenomena of the change of the spectral line shape and line width with dilution were observed for the air/DMSO aqueous solution interfaces.

HR-BB-SFG-VS of air/DMSO aqueous solution interface. SFG spectra of Air/DMSO is measured to benchmark this new sub-1 cm^{-1} HR-BB-SFG-VS instrumentation (Figure 4A). The spectrum of air/neat DMSO interface in the *ssp* polarization combination, with *s* the SFG signal polarization, *s*

the visible polarization, and *p* the IR polarization, respectively, is nearly with the same lineshape as the air/neat DMSO spectrum with the 1 kHz sub-1 cm^{-1} HR-BB-SFG-VS measurement reported previously.[10] Here, *s* denotes the polarization perpendicular to the visible and IR incident plane, and *p* the polarization in the incident plane. The FWHM of the peak centered at 2916.5 ± 0.1 cm^{-1} is 8.7 ± 0.1 cm^{-1}, in comparison to that of 2916.88 ± 0.07 cm^{-1} and FWHM = 8.8 ± 0.1 cm^{-1} reported previously.[10] These values agree with each other within less than 0.1 cm^{-1}. The visible frequency in this work is about 517 nm, i.e. SFG signal is around 450 nm; while that of the 1 kHz system was about 800 nm, i.e. SFG signal around 650 nm. The spectra resolution using the same spectrograph, grating, slit width and CCD camera is lower for the 450 nm region than that of the 650 nm region, with a factor of $(650/450)^2 = 2.1$. Therefore, the SFG spectra lineshape in this new sub-1 cm^{-1} HR-BB-SFG-VS can be improved by using spectrograph with higher spectral resolution in the future.

Also measured are twelve spectra for the air/DMSO aqueous solution interfaces, with the mole fraction of DMSO changed from 0.90 to 0.01. These spectra showed a monotonic blue shift of the peak position and reduction of the peak intensity with the decreasing of the DMSO bulk concentration. In addition, the FWHM of the peak also reduced monotonically with the decreasing of DMSO concentration, i.e., from FWHM = 8.7 ± 0.1 cm^{-1} at 2916.6 ± 0.1 cm^{-1} with x = 1.0 to FWHM = 4.4 ± 0.2 cm^{-1} at 2925.8 ± 0.2 cm^{-1} peak with x = 0.01. The peak positions, FWHMs and amplitudes fit with a Lorentzian lineshape are listed in Table II. Similar peak shift was observed before for the air/DMSO aqueous interfaces with lower spectral resolution; while such FWHM change was not possible with a spectral resolution of 17 cm^{-1} of the SFG spectrometer used.[45] Such significant change of FWHM by 4.3 cm^{-1} from 8.7 to 4.4 cm^{-1} over 12 concentrations can only be accurately monitored with the excellent spectral resolution and accurate lineshape made possible with the sub-1 cm^{-1} HR-BB-SFG-VS. The decrease of the FWHM of the ~2917 cm^{-1} peak from 8.7 to 4.4 cm^{-1} with the dilution of DMSO with water is surprising, which is also a unique phenomenon for the air/DMSO aqueous interfaces. In the DMSO aqueous bulk solution, this peak actually became broader with dilution.[46-47] It is known that the ~2917 cm^{-1} peak of the air/neat DMSO interface, appearing to be a

nice single peak, actually contains two closely overlapping peaks separated by about 2.7 cm^{-1} with their respective central wavelengths, which were first observed and resolved with the 1 kHz sub-1 cm^{-1} HR-BB-SFG-VS a decade ago.[10] The importance of such data is that they provide explicit new evidence of the subtle interactions and conformational changes at the liquid interface. What happened to these two overlapping peaks is under further investigation for future report. Nevertheless, these new data of the air/DMSO aqueous solution interfaces with the 100 kHz sub-1 cm^{-1} HR-BB-SFG-VS suggest unique detailed structural and interaction changes at these interfaces. It also explicitly suggests that the new opportunities from the sub-1 cm^{-1} HR-BB-SFG-VS experimental measurement require more accurate theoretical understanding, not only on the simple liquid interfaces, but also on the complicated material and biological interfaces as well.

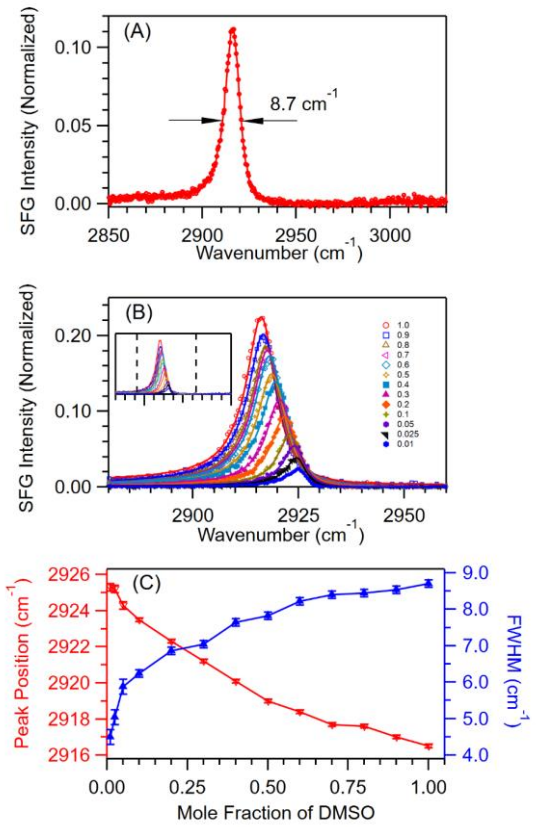

Figure 4. The *ssp* polarization HR-BB-SFG vibrational spectra of -CH_3 symmetric stretching of DMSO molecules at the air/ DMSO aqueous solution interface (mole fraction x = 1.0, i.e. pure DMSO, to x= 0.01, diluted 100 times). **Panel (A)**: *ssp* polarization HR-BB-SFG vibrational spectra of -CH_3 symmetric stretching of DMSO molecules at the air/ DMSO aqueous solution interface. **Panel (B)**: *ssp* spectra of the air/DMSO aqueous solution interfaces (mole fraction x = 1.0, i.e. pure DMSO, to x= 0.01, diluted 100 times). The insert figure are spectra without expanding the x-axis. **Panel (C)**: Peak position and linewidth (FWHM) with Lorentzian fittings of the spectra in **Panel (B)**. HR-BB-SFG-VS successfully captured the gradual spectral blue shift and the band width reduction with dilution. For example, FWHM = 4.4 ± 0.2 cm^{-1} at 2925.8 ± 0.2 cm^{-1} peak with x = 0.01, and FWHM = 8.7 ± 0.1

cm^{-1} at 2916.6 ± 0.1 cm^{-1} with x = 1.0, respectively.

Table II. The *ssp* polarization HR-BB-SFG vibrational spectra of -CH_3 symmetric stretching of DMSO molecules at the air/ DMSO aqueous solution interface parameters in Figure 4.

DMSO Mole fraction	Position (cm^{-1})	FWHM (cm^{-1})	Lorentzian Amplitude
1.00	2916.5 ± 0.1	8.7 ± 0.1	0.112 ± 0.005
0.90	2917.1 ± 0.1	8.5 ± 0.1	0.099 ± 0.005
0.80	2917.6 ± 0.1	8.4 ± 0.1	0.093± 0.005
0.70	2917.7 ± 0.1	8.3 ± 0.1	0.092± 0.005
0.60	2918.4 ± 0.1	8.2 ± 0.1	0.086± 0.005
0.50	2919.0 ± 0.1	7.8 ± 0.1	0.075± 0.005
0.40	2920.1 ± 0.1	7.6 ± 0.1	0.068± 0.005
0.30	2921.2 ± 0.1	7.0 ± 0.1	0.058± 0.005
0.20	2922.3 ± 0.1	6.9 ± 0.1	0.046± 0.005
0.10	2923.5 ± 0.1	6.2 ± 0.1	0.035± 0.005
0.05	2924.3 ± 0.1	5.9 ± 0.1	0.026± 0.007
0.025	2925.2 ± 0.2	5.1 ± 0.2	0.020± 0.007
0.01	2925.3 ± 0.2	4.4 ± 0.2	0.012± 0.007

Control of Heating Effects. Controlling of the focus of the visible and the IR beams at the air/DMSO interface is crucial for obtaining SFG signal with enough sensitivity and for making sure the SFG signal is not subjected to the accumulative heating effects near the surface, particularly from the absorbing IR beam. Surface heating in the region near the liquid interface has been a known issue in SFG measurement.[30-31]

Figure 5 shows the HR-BB-SFG-VS spectra of the CH_3- groups from the air/DMSO surface results with the same visible (~750 mW at 517.36 nm @ 100 kHz) and IR (~190 mW centered at 2910 cm^{-1} @100 kHz) powers under two sets of focusing conditions and each at four repetition rates, i.e. 100, 50, 33 and 10 kHz, respectively. The visible or the IR power is reduced proportionally when the repetition rate is reduced in the range of 100 to 10 kHz. The spectra in Panel A used a focal lens of FL = 250 mm for the visible beam and FL = 45 mm for the IR beam, and the focusing point is on the interface. This set of spectra has significantly higher noise level and the spectral width also changes significantly with the repetition rate, as shown on the plot in Panel C and D, while the peak position remains roughly the same. Lowering the repetition rate delivers lower total power of both visible and IR beams at the interface, resulting in lower signal intensity. The peak intensity is reduced

from about 10 counts per second (1200 counts/120 second shown in Panel A at 100 kHz, to about 2 counts per second at 10 kHz; and the S/N ratio is reduced from about 23:1 to about 8:1; while the spectral FWHM is from 9.7 ± 0.2 cm^{-1} to 8.5 ± 0.4 cm^{-1}. Such power dependence of the spectral SNR and particularly the FWHM values is due the heating of the sample. By reducing the laser power density at the solution interface, particularly for the IR beam, such effects are effectively eliminated, as shown in Panel B. The spectra in Panel B used a focal lens of FL = 270 mm for the visible beam and FL = 60 mm for the IR beam, and the focusing point of each beam is moved 10 to 20 mm above the liquid interface to avoid direct heating of the liquid phase. With this adjustment, the spot size of the visible beam at the interface is kept larger than that of the IR beam. In comparison to the data in Panel A, the noise level of spectra in Panel B is significantly reduced, and the SNR is improved, e.g. to 120:1 at 100 kHz and 40:1 at 10 kHz with the same visible and IR power. Most importantly, the FWHM of the spectra at different repetition rate remained unchanged as 8.7 ± 0.1 cm^{-1} for all these rates. The 100 kHz spectrum also shows that the peak intensity at ~ 2917 cm^{-1} is as high as 23 counts per second (2800 counts per 120 seconds), which is about 3 times of that from the same air/DMSO interface measured with the 1 kHz sub-1 cm^{-1} HR-BB-SFG-VS reported previously.[10] This signal sensitivity still has room for improvement with the change of laser power and with careful controlling of the focusing and overlapping conditions of the visible and IR beams.

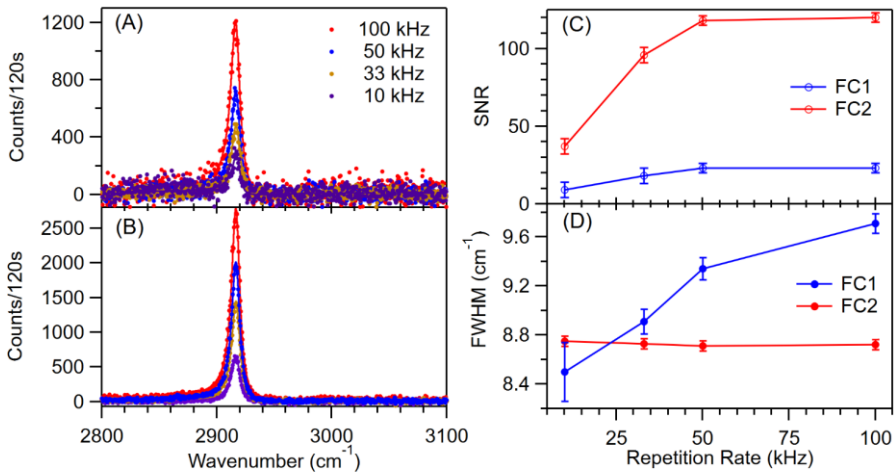

Figure 5. The HR-BB-SFG-VS spectra of air/DMSO interface in the C−H stretching region measured at different laser repetition-rates at 10 kHz, 33 kHz, 50 kHz and 100 kHz, respectively. These are the raw spectra, i.e. they are not normalized to the signal from the z-cut quartz crystal surface. **Panel (A):** The air/DMSO surface with VIS (FL:

250 mm) and IR (FL: 45 mm) of focusing condition 1 (FC1). **Panel (B)**: The air/DMSO surface with VIS (FL: 270 mm) and IR (FL: 60 mm) of focusing condition 2 (FC2). **Panel (C)**: The calculated signal-to-noise ratio and **Panel (D)**: peak position and spectra linewidth FWHM of with two focusing conditions (FC1 and FC2) at 10 kHz, 33 kHz, 50 kHz and 100 kHz, respectively.

HR-BB-SFG-VS spectrum of the air/D_2O interface. Figure 6 shows the 100 kHz sub-1 cm^{-1} HR-BB-SFG-VS spectra of the air/neat D_2O interface in the O-D stretching region. This is the first report on the sub-1 cm^{-1} HR-BB-SFG-VS spectra of the air/neat D_2O interface. The spectrum was patched together from tree spectra with different central frequencies of the IR beam. In these three spectra, the power of the visible beam is ~ 900 mW, and the power of the IR beam is 150 mW for the three central frequencies, i.e. 2900, 2700 and 2500 cm^{-1}, respectively. In comparison to the BB-SFG-VS spectra of the air/D_2O interface with lower spectral resolution (usually with spectral resolution larger than 10 cm^{-1}),[48-51] the spectrum reported here has less noise and improved lineshape. Here, the peak intensity of the free O-D peak at ~ 2740 cm^{-1} is about 20% higher than that of the hydrogen-bonded peak ~ 2490 cm^{-1}; while in previous BB-SFG-VS spectra, the free O-D peak intensity is in general lower or not higher than that of the hydrogen-bonded peak. This is the preliminary report on the HR-BB-SFG-VS spectrum of the air/D_2O interface. Improved and systematic measurement on the air/D_2O and air/H_2O HR-BB-SFG-VS spectra is underway in our laboratory, with the addition of the purge for CO_2 and H_2O in the IR beam path.

It is known that the SFG signal of the air/H_2O and air/D_2O interfaces are among the smallest of the liquid interfaces. In Figure 6, the intensity of the free O-D peak at ~2740 cm^{-1} is about 1.1 x 10^{-4} as normalized to the SFG signal reflected from the z-cut quartz crystal surface, which is about 1000 times smaller than that of the 2917 cm^{-1} peak of the air/neat DMSO interface spectrum, i.e. about 0.11 normalized, as in Figure 4. Here, no apparent heating effect in the spectrum of the air/D_2O interface was observed with the same focusing condition as in the measurement of the air/DMSO interface. The success to measure the SFG spectrum of the air/D_2O interface with good spectral quality indicates that this 100 kHz sub-1 cm^{-1} HR-BB-SFG-VS spectrometer is broadly applicable to studies of molecular interfaces, even with several orders smaller SFG signal than that of the air/DMSO interface.

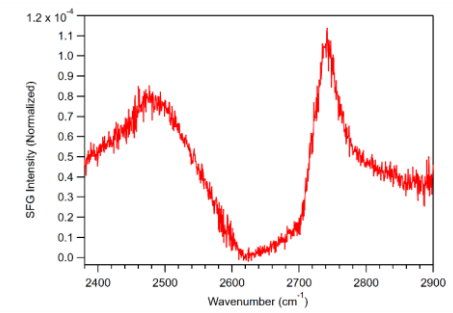

Figure 6. Sub-1 cm^{-1} HR-BB-SFG-VS spectra of the air/D_2O interface in *ssp* polarization combination. The D_2O signal was acquired over 60 minutes, and it is normalized to the reference signal of the thick z-cut quartz crystal, which was acquired over 30 seconds. The spectrum below 2400 cm^{-1} is not presented as the IR beam is not purged to avoid the significant IR absorption by the ambient CO_2 in the IR beam path.

4. Conclusions

In summary, a 100 kHz sub-1 cm^{-1} high-resolution broadband sum frequency generation vibrational spectrometer (HR-BB-SFG-VS) is successfully built for broad applications in molecular interface studies. This sub-1 cm^{-1} high-resolution spectrometer is based on the OPA and SHBC unit pumped by a single femtosecond laser source, without complicated and costly systems, such as the synchronization of two laser amplifiers,[10] or the system with two amplifiers with different pulse widths using a common seed pulses.[25, 29] Data from the air/DMSO aqueous solution interface and air/D_2O interfaces show that the heating effect from 100 kHz laser can be effectively managed through control of the focusing conditions of the visible and IR beams, and the sensitivity of the spectra with high SNR and high-quality lineshape can be effectively achieved. This low-cost, space saving, and relatively easy to construct high-repetition rate sub-1 cm^{-1} HR-BB-SFG-VS system can be easily adopted in many academic and research laboratories, and it may gradually phase-out the currently widely used more costly conventional BB-SFG-VS systems, associated with significantly lower spectral resolution and more significant spectral distortion.[11]

For interfaces with non-doubly resonant SFG-VS, such as the air/DMSO interface, the spectrum taken with this 100 kHz sub-1 cm^{-1} HR-BB-SFG-VS system with ~517nm visible wavelength is almost identical with the spectrum from the 1 kHz sub-1 cm^{-1} HR-BB-SFG-VS using 800 nm visible wavelength.[10] For interface that is doubly-resonant (DR),[52-53] tunability of the visible wavelength in a broad range is required. Several approaches to generate tunable sub-1 cm^{-1} pulses in different visible

wavelength are possible. Using CVBG-SHBC with different center wavelengths after a tunable OPA with enough power is one; while another possibility is to pump a narrow band OPA with the sub-1 cm^{-1} pulses generated from the CVBG-SHBC. Here, the picosecond amplifier in the 1 kHz sub-1 cm^{-1} HR-BB-SFG-VS system using the synchronized ps-fs amplifiers has enough power to pump narrow band OPA in generating sub-1 cm^{-1} pulses in the visible region. Despite its disadvantage with high-cost and the demand for significantly more space, the approach with synchronization of ps-fs amplifiers for sub-1 cm^{-1} HR-BB-SFG-VS is still valuable and irreplaceable for many advanced applications. Finally, with high-power fiber lasers at higher repetitions rate, multiple OPAs can be used to generate sub-100 fs pulses tunable in the broad IR and visible ranges. Combining with the CVBG-SHBC approach to generate sub-1 cm^{-1} visible pulses, it is readily feasible to develop other broad band pump-probe and multi-dimensional nonlinear spectroscopies, with sub-1 cm^{-1} spectral resolution and sub 100 fs time resolution, such as multi-dimensional SFG-VS, femtosecond stimulated Raman spectroscopy (FSRS), and coherent anti-Stokes Raman spectroscopy (CARS), etc. At any rate, with the successful measurement on the liquid interfaces reported here, now the sub-1 cm^{-1} HR-BB-SFG-VS is also in the 100 kHz era. With such development, many new discoveries will follow.

AUTHOR INFORMATION

Corresponding Author

*(H.-F. Wang) E-mail: wanghongfei@westlake.edu.cn

First Author

(J.-M. Cao) E-mail: caojingming@westlake.edu.cn

Other Authors

(A.-A. Liu) E-mail: liuaa@baqis.ac.cn

(S.-Y. Yang) E-mail: yangshuyi@westlake.edu.cn

(X.-X. Peng) E-mail: pengxingxing@westlake.edu.cn

ORCID

Jing-Ming Cao: 0009-0007-6395-5516

An-An Liu: 0009-0001-8191-6111

Shu-Yi Yang: 0009-0000-9138-4609

Xing-Xing Peng: 0000-0003-1468-2770

Hong-Fei Wang: 0000-0001-8238-1641

Notes

The authors declare no competing financial interest.

ACKNOWLEDGMENTS

This work was supported by the National Natural Science Foundation of China (NSFC Grant No. 21727802) and Westlake Education Foundation.

References

1. Zhu, X. D.; Suhr, H.; Shen, Y. R., Surface Vibrational Spectroscopy by Infrared-Visible Sum Frequency Generation. *Physical Review B* **1987**, *35*, 3047-3050.
2. Eisenthal, K. B., Liquid Interfaces Probed by Second-Harmonic and Sum-Frequency Spectroscopy. *Chemical Reviews* **1996**, *96*, 1343-1360.
3. Miranda, P. B.; Shen, Y. R., Liquid Interfaces: A Study by Sum-Frequency Vibrational Spectroscopy. *The Journal of Physical Chemistry B* **1999**, *103*, 3292-3307.
4. Wang, H.-F., Sum Frequency Generation Vibrational Spectroscopy (SFG-VS) for Complex Molecular Surfaces and Interfaces: Spectral Lineshape Measurement and Analysis Plus Some Controversial Issues. *Progress in Surface Science* **2016**, *91*, 155-182.
5. Zhuang, X.; Miranda, P. B.; Kim, D.; Shen, Y. R., Mapping Molecular Orientation and Conformation at Interfaces by Surface Nonlinear Optics. *Physical Review B* **1999**, *59*, 12632-12640.
6. Wang, H.-F.; Gan, W.; Lu, R.; Rao, Y.; Wu, B.-H., Quantitative Spectral and Orientational Analysis in Surface Sum Frequency Generation Vibrational Spectroscopy (SFG-VS). *International Reviews in Physical Chemistry* **2005**, *24*, 191-256.
7. Wang, H.-F.; Velarde, L.; Gan, W.; Fu, L., Quantitative Sum-Frequency Generation Vibrational Spectroscopy of Molecular Surfaces and Interfaces: Lineshape, Polarization, and Orientation. *Annual Review of Physical Chemistry* **2015**, *66*, 189-216.
8. Shen, Y. R., Phase-Sensitive Sum-Frequency Spectroscopy. *Annual Review of Physical Chemistry* **2013**, *64*, 129-150.
9. Yamaguchi, S.; Otosu, T., Progress in Phase-Sensitive Sum Frequency Generation Spectroscopy. *Physical Chemistry Chemical Physics* **2021**, *23*, 18253-18267.
10. Velarde, L.; Zhang, X.-Y.; Lu, Z.; Joly, A. G.; Wang, Z.; Wang, H.-F., Communication: Spectroscopic Phase and Lineshapes in High-Resolution Broadband Sum Frequency Vibrational Spectroscopy: Resolving Interfacial Inhomogeneities of “Identical” Molecular Groups. *The Journal*

of Chemical Physics **2011**, *135*, 241102.
11. Wang, H.; Hu, X.-H.; Wang, H.-F., Temporal and Chirp Effects of Laser Pulses on the Spectral Line Shape in Sum-Frequency Generation Vibrational Spectroscopy. *The Journal of Chemical Physics* **2022**, *156*, 204706.
12. Hess, C.; Wolf, M.; Roke, S.; Bonn, M., Femtosecond Time-Resolved Vibrational SFG Spectroscopy of Co/Ru (001). *Surface Science* **2002**, *502*, 304-312.
13. Ishibashi, T.-A.; Onishi, H., Vibrationally Resonant Sum-Frequency Generation Spectral Shape Dependent on the Interval between Picosecond-Visible and Femtosecond-Infrared Laser Pulses. *Chemical Physics Letters* **2001**, *346*, 413-418.
14. Noguchi, H.; Okada, T.; Onda, K.; Kano, S.; Wada, A.; Domen, K., Time-Resolved SFG Study of Formate on a Ni (111) Surface under Irradiation of Picosecond Laser Pulses. *Surface Science* **2003**, *528*, 183-188.
15. Richter, L. J.; Petralli-Mallow, T. P.; Stephenson, J. C., Vibrationally Resolved Sum-Frequency Generation with Broad-Bandwidth Infrared Pulses. *Optics Letters* **1998**, *23*, 1594-1596.
16. Smith, J. P.; Hinson-Smith, V., Product Review: SFG Coming of Age. **2004**, *76*, 287A.
17. Star, D.; Kikteva, T.; Leach, G. W., Surface Vibrational Coherence at the CaF_2/Air Interface: Vibrational Wave Packet Dynamics as a Probe of Interface Inhomogeneity. *The Journal of chemical physics* **1999**, *111*, 14-17.
18. Wang, J.; Dubost, H.; Ghalgaoui, A.; Zheng, W.; Carrez, S.; Ouvrard, A.; Bourguignon, B., Effect of Visible Pulse Shaping on the Accuracy of Relative Intensity Measurements in BBSFG Vibrational Spectroscopy. *Surface Science* **2014**, *626*, 26-39.
19. Velarde, L.; Wang, H.-F., Unified Treatment and Measurement of the Spectral Resolution and Temporal Effects in Frequency-Resolved Sum-Frequency Generation Vibrational Spectroscopy (SFG-VS). *Physical Chemistry Chemical Physics* **2013**, *15*, 19970-19984.
20. Li, Y.; Feng, R.; Lin, L.; Liu, M.; Guo, Y.; Zhang, Z., Ordering Effects of Cholesterol on Sphingomyelin Monolayers Investigated by High-Resolution Broadband Sum-Frequency Generation Vibrational Spectroscopy. *Chinese Chemical Letters* **2018**, *29*, 357-360.
21. Hommel, E. L.; Ma, G.; Allen, H. C., Broadband Vibrational Sum Frequency Generation Spectroscopy of a Liquid Surface. *Analytical Sciences* **2001**, *17*, 1325-1329.
22. Liljeblad, J. F.; Tyrode, E., Vibrational Sum Frequency Spectroscopy Studies at Solid/Liquid Interfaces: Influence of the Experimental Geometry in the Spectral Shape and Enhancement. *The Journal of Physical Chemistry C* **2012**, *116*, 22893-22903.
23. Ma, G.; Liu, J.; Fu, L.; Yan, E. C., Probing Water and Biomolecules at the Air–Water Interface with a Broad Bandwidth Vibrational Sum Frequency Generation Spectrometer from 3800 to 900 cm^{-1}. *Applied Spectroscopy* **2009**, *63*, 528-537.
24. Weeraman, C.; Mitchell, S. A.; Lausten, R.; Johnston, L. J.; Stolow, A., Vibrational Sum Frequency Generation Spectroscopy Using Inverted Visible Pulses. *Optics Express* **2010**, *18*, 11483-11494.
25. Zhang, R.; Peng, X.; Jiao, Z.; Luo, T.; Zhou, C.; Yang, X.; Ren, Z., Flexible High-Resolution Broadband Sum-Frequency Generation Vibrational Spectroscopy for Intrinsic Spectral Line Widths. *The Journal of Chemical Physics* **2019**, *150*, 074702.
26. Ge, A.; Kastlunger, G.; Meng, J.; Lindgren, P.; Song, J.; Liu, Q.; Zaslavsky, A.; Lian, T.; Peterson, A. A., On the Coupling of Electron Transfer to Proton Transfer at Electrified Interfaces. *Journal of the American Chemical Society* **2020**, *142*, 11829-11834.
27. Yesudas, F.; Mero, M.; Kneipp, J.; Heiner, Z., Vibrational Sum-Frequency Generation

Spectroscopy of Lipid Bilayers at Repetition Rates up to 100 kHz. *The Journal of Chemical Physics* **2018**, *148*, 104702.
28. Yesudas, F.; Mero, M.; Kneipp, J.; Heiner, Z., High-Resolution and High-Repetition-Rate Vibrational Sum-Frequency Generation Spectroscopy of One- and Two-Component Phosphatidylcholine Monolayers. *Analytical and Bioanalytical Chemistry* **2019**, *411*, 4861-4871.
29. Kananavičius, R.; Danilevičius, R.; Januškevičius, R.; Madeikis, K.; Lukošiūnas, J. In *Broadband High Resolution Sum Frequency Generation Spectrometer for Molecular Vibrational Spectroscopy at Interfaces*, Nonlinear Frequency Generation and Conversion: Materials and Devices XXII, SPIE: 2023; pp 38-45.
30. Xu, Y.; Wang, R.; Ma, S.; Zhou, L.; Shen, Y. R.; Tian, C., Theoretical Analysis and Simulation of Pulsed Laser Heating at Interface. *Journal of Applied Physics* **2018**, *123*, 025301.
31. Backus, E. H.; Bonn, D.; Cantin, S.; Roke, S.; Bonn, M., Laser-Heating-Induced Displacement of Surfactants on the Water Surface. *The Journal of Physical Chemistry B* **2012**, *116*, 2703-2712.
32. Heiner, Z.; Petrov, V.; Mero, M., Compact, High-Repetition-Rate Source for Broadband Sum-Frequency Generation Spectroscopy. *APL Photonics* **2017**, *2*, 066102.
33. Wei, F.; Urashima, S.-h.; Nihonyanagi, S.; Tahara, T., Elucidation of the PH-Dependent Electric Double Layer Structure at the Silica/Water Interface Using Heterodyne-Detected Vibrational Sum Frequency Generation Spectroscopy. *Journal of the American Chemical Society* **2023**.
34. Mifflin, A. L.; Velarde, L.; Ho, J.; Psciuk, B. T.; Negre, C. F.; Ebben, C. J.; Upshur, M. A.; Lu, Z.; Strick, B. L.; Thomson, R. J., Accurate Line Shapes from Sub-1 cm^{-1} Resolution Sum Frequency Generation Vibrational Spectroscopy of A-Pinene at Room Temperature. *The Journal of Physical Chemistry A* **2015**, *119*, 1292-1302.
35. Zhu, L.; Liu, W.; Wang, Y.; Fang, C., Sum-Frequency-Generation-Based Laser Sidebands for Tunable Femtosecond Raman Spectroscopy in the Ultraviolet. *Applied Sciences* **2015**, *5*, 48-61.
36. Chen, S.-L.; Fu, L.; Gan, W.; Wang, H.-F., Homogeneous and Inhomogeneous Broadenings and the Voigt Line Shapes in the Phase-Resolved and Intensity Sum-Frequency Generation Vibrational Spectroscopy. *The Journal of Chemical Physics* **2016**, *144*, 034704.
37. Fu, L.; Chen, S.-L.; Wang, H.-F., Validation of Spectra and Phase in Sub-1 cm^{-1} Resolution Sum-Frequency Generation Vibrational Spectroscopy through Internal Heterodyne Phase-Resolved Measurement. *The Journal of Physical Chemistry B* **2016**, *120*, 1579-1589.
38. Hu, X.-H.; Fu, L.; Hou, J.; Zhang, Y.-N.; Zhang, Z.; Wang, H.-F., N–H Chirality in Folded Peptide Lk7$_{\beta}$ Is Governed by the Cα–H Chirality. *The Journal of Physical Chemistry Letters* **2020**, *11*, 1282-1290.
39. Velarde, L.; Wang, H.-F., Capturing Inhomogeneous Broadening of the –CN Stretch Vibration in a Langmuir Monolayer with High-Resolution Spectra and Ultrafast Vibrational Dynamics in Sum-Frequency Generation Vibrational Spectroscopy (SFG-VS). *The Journal of Chemical Physics* **2013**, *139*, 084204.
40. Belai, O.; Podivilov, E.; Shapiro, D., Group Delay in Bragg Grating with Linear Chirp. *Optics Communications* **2006**, *266*, 512-520.
41. João, C.; Pires, H.; Cardoso, L.; Imran, T.; Figueira, G., Dispersion Compensation by Two-Stage Stretching in a Sub-400 fs, 1.2 μJ Yb: CaF_2 Amplifier. *Optics Express* **2014**, *22*, 10097-10104.
42. Nejbauer, M.; Kardaś, T. M.; Stepanenko, Y.; Radzewicz, C., Spectral Compression of Femtosecond Pulses Using Chirped Volume Bragg Gratings. *Optics Letters* **2016**, *41*, 2394-2397.
43. Heiner, Z.; Wang, L.; Petrov, V.; Mero, M., Broadband Vibrational Sum-Frequency Generation Spectrometer at 100 kHz in the 950-1750 cm^{-1} Spectral Range Utilizing a $LiGaS_2$ Optical Parametric

Amplifier. *Optics Express* **2019**, *27*, 15289-15297.
44. Hu, X.-H.; Wei, F.; Wang, H.; Wang, H.-F., α-Quartz Crystal as Absolute Intensity and Phase Standard in Sum-Frequency Generation Vibrational Spectroscopy. *The Journal of Physical Chemistry C* **2019**, *123*, 15071-15086.
45. Allen, H. C.; Gragson, D.; Richmond, G., Molecular Structure and Adsorption of Dimethyl Sulfoxide at the Surface of Aqueous Solutions. *The Journal of Physical Chemistry B* **1999**, *103*, 660-666.
46. Singh, S.; Srivastava, S. K.; Singh, D. K., Raman Scattering and DFT Calculations Used for Analyzing the Structural Features of DMSO in Water and Methanol. *RSC Advances* **2013**, *3*, 4381-4390.
47. Yang, B.; Cao, X.; Wang, C.; Wang, S.; Sun, C., Investigation of Hydrogen Bonding in Water/DMSO Binary Mixtures by Raman Spectroscopy. *Spectrochimica Acta Part A: Molecular and Biomolecular Spectroscopy* **2020**, *228*, 117704.
48. Tian, C.-S.; Shen, Y. R., Isotopic Dilution Study of the Water/Vapor Interface by Phase-Sensitive Sum-Frequency Vibrational Spectroscopy. *Journal of the American Chemical Society* **2009**, *131*, 2790-2791.
49. Sovago, M.; Campen, R. K.; Bakker, H. J.; Bonn, M., Hydrogen Bonding Strength of Interfacial Water Determined with Surface Sum-Frequency Generation. *Chemical Physics Letters* **2009**, *470*, 7-12.
50. Strazdaite, S.; Versluis, J.; Backus, E. H.; Bakker, H. J., Enhanced Ordering of Water at Hydrophobic Surfaces. *The Journal of Chemical Physics* **2014**, *140*, 054711.
51. Piatkowski, L.; Zhang, Z.; Backus, E. H.; Bakker, H. J.; Bonn, M., Extreme Surface Propensity of Halide Ions in Water. *Nature Communications* **2014**, *5*, 4083.
52. Raschke, M.; Hayashi, M.; Lin, S.; Shen, Y., Doubly-Resonant Sum-Frequency Generation Spectroscopy for Surface Studies. *Chemical Physics Letters* **2002**, *359*, 367-372.
53. Wu, D.; Deng, G.-H.; Guo, Y.; Wang, H.-F., Observation of the Interference between the Intramolecular IR−Visible and Visible−IR Processes in the Doubly Resonant Sum Frequency Generation Vibrational Spectroscopy of Rhodamine 6G Adsorbed at the Air/Water Interface. *The Journal of Physical Chemistry A* **2009**, *113*, 6058-6063.